Three Pulse Photon Echoes on an Inhomogeneously Stark Broadened Line at 3 mm-Wavelengths *

F. Rohart and B. Macke
Laboratoire de Spectroscopie Hertzienne, Associé au CNRS, Université de Lille

Z. Naturforsch. **36a**, 929–936 (1981); received July 6, 1981

Three pulse photon echoes are studied when the prevailing inhomogeneous damping arises from the application of an inhomogeneous Stark field. Whereas the molecular free flight through the inhomogeneous Stark field entails a strong attenuation of conventional photon echoes, this effect is shown to be eliminated for the even numbered echoes of a Carr Purcell sequence. These predictions are well supported by a detailed experimental study at a 3 mm wavelength. Velocity changing collision influence is discussed and T_1 and T_2 relaxation times of the $(J, |KM| = 1,1 \rightarrow 2,1)$ rotational transition of CH_3F are incidentally determined.

I. Introduction

Since the pioneering work of Kurnit et al. [1] on a solid state sample, photon echoes have been observed on dilute gases independently by Jenkins and Wagner [2], Patel and Slusher [3], and Bölger and Diels [4]. These echoes result from the coherent excitation of an ensemble of two level systems, and are analogous to the nuclear spin echoes [5]. A first resonant strong laser pulse ("$\pi/2$ pulse") induces a maximum of coherence of the gas which then evolves freely (optical precession). Due to inhomogeneous dephasing (e.g. Doppler effect or spatial inhomogeneities), the macroscopic polarization is quickly destroyed though the gas is not at thermal equilibrium; the dephasing is then inverted at time T, using a second laser pulse ("π pulse") and the macroscopic coherence builds up again to lead to an echo at time $2T$.

The photon echo technique appears then very fruitful to pick out phenomena selectively which are hidden by large inhomogeneous dampings. For this purpose, more specific sequences such as Carr Purcell echoes [6, 7] and three pulse photon echoes [8, 9] have revealed to be interesting tools, and information has been obtained about strong and weak collisions, including phase and velocity changing collisions [7, 10]. A wide variety of experimental schemes have been developed, for the optical as well as the I.R. and the microwave domains. They include electromagnetic pulses of various polarization and propagation directions, Stark switching, frequency and phase switching ([8, 11] and references therein).

In this paper, we report a three pulse photon echo experiment in the millimeter range. This domain is characterized by a moderate Doppler broadening associated to large dipole moment matrix elements: the whole Doppler profile is easily saturated, and simple models for molecule-field interaction can be developed. On the other hand, in contrast with population relaxation, coherence relaxation is not easily determined: the Doppler damping is too fast for reliable optical precession measurements and too slow for photon echo experiments as well [12]. The latter requirement was overcome by switching the absorption with an inhomogeneous Stark field [13] involving a fast damping of the optical precession. However, the observed two pulse photon echoes exhibited a large extradamping related to molecular motions through the inhomogeneous Stark field. Although this situation looks similar to pulsed NMR experiments in inhomogeneous magnetic fields [5, 6], it contrasts strongly since, instead of a Brownian motion, molecules are in the free flight regime and only few and weak velocity changing collisions occur [7]. In such conditions, the echo damping related to molecular motions does not have necessarily an irreversible character, and it may exist pulse sequences leading to an exact rephasing of microscopic coherences. We show in Sect. II that, in the case of a Carr Purcell sequence, these free flight effects in the inhomogeneous Stark field are removed for the even numbered echoes which only depend on coherence

* A preliminary report of this work has been given at the 35th Symposium on Molecular Structure and Spectroscopy, Columbus, Ohio, June 1980.

Reprint requests to Dr F. Rohart, Laboratoire de Spectroscopie Hertzienne, Université de Lille I, 59655 Villeneuve d'Ascq Cedex, France.

0340-4811 / 81 / 0900-0929 $ 01.00/0. — Please order a reprint rather than making your own copy.

relaxation. This property of Carr Purcell sequence is experimentally demonstrated in Section III. To conclude (Sect. IV), applications to velocity changing collision studies are discussed and we derive independently the population and coherence relaxation times T_1 and T_2 for the $(J, |K M| = 1, 1 \rightarrow 2, 1)$ line of CH_3F.

II. Experimental Principle

The principle and basic properties of a three pulse photon echo experiment have been extensively reviewed by Shoemaker [8], so we only study the specific case of an inhomogeneous damping induced mainly by a strongly inhomogeneous Stark field.

We consider a gas of two level systems characterized by the eigenfrequency ω_{00}, the dipole moment matrix element μ and the time T_1 (resp. T_2) characterizing the population (resp. coherence) relaxation. The gas is continuously irradiated by a plane electromagnetic wave, propagating along the $z'z$ axis, the frequency of which ω coincides with the zero Stark field line frequency ω_{00}. Excitation pulses, performed by the Stark switching technique, are assumed to be exactly resonant: this implies that the residual inhomogeneous broadening due to the Doppler effect is negligible with respect to the saturation broadening. Optical precession occurs when the gas is switched out of resonance by the inhomogeneous Stark field; the precession frequency in the rotating frame is then $\alpha = \omega - \omega_0$, where the eigenfrequency ω_0 now depends strongly on molecular locations and varies according to molecular motions. The Stark field distribution may be characterized by that of α. Let us denote $\bar{\alpha}$ its mean value and G its gradient assumed to be uniform along the $y'y$ direction. If b is the y dimension of the cell, $G\,b$ is then simply the total inhomogeneity of α. As long as velocity changing collisions may be neglected, the value of α for a molecule located in y at time $t = 0$ with velocity components v_y (resp. v_z) along the y (resp. z) axis can be written as:

$$\alpha(t) = \bar{\alpha} - k v_z + G y + G v_y t, \tag{1}$$

where k is the propagation constant ω/c.

The gas, initially at thermal equilibrium, is submitted to the Stark sequence of Figure 1. Since we are primarily concerned in echo amplitude behaviours versus delay times, we mostly take an interest in precession phase calculations. So we neglect relaxation processes during excitation pulses which are assumed much shorter than relaxation times T_1 and T_2 and, at the moment, we do not take an exact account of pulse areas which only affect absolute echo amplitudes [8].

The first Stark pulse (duration t_1) induces a strong coherence at time $t = 0$. For a given molecular class, the phase φ_{0p} of the optical precession following this preparation is written, in the rotating frame, as:

$$\varphi_{0p}(t) = \int_0^t \alpha(t')\,dt' = \bar{\alpha}\,t + (-k v_z + G y)\,t + G v_y t^2/2, \tag{2}$$

where $\Phi_i = (-k v_z + G y)\,t$ is the phase deviation related to the inhomogeneous effects and $\Phi_m = G v_y t^2/2$ is the phase deviation related to molecular motion in the Stark field. Φ_i is the main cause of the damping of the macroscopic polarization: when the Stark broadening prevails over the Doppler broadening, the damping caracteristic time is $\cong (2\pi/G\,b)$ [13].

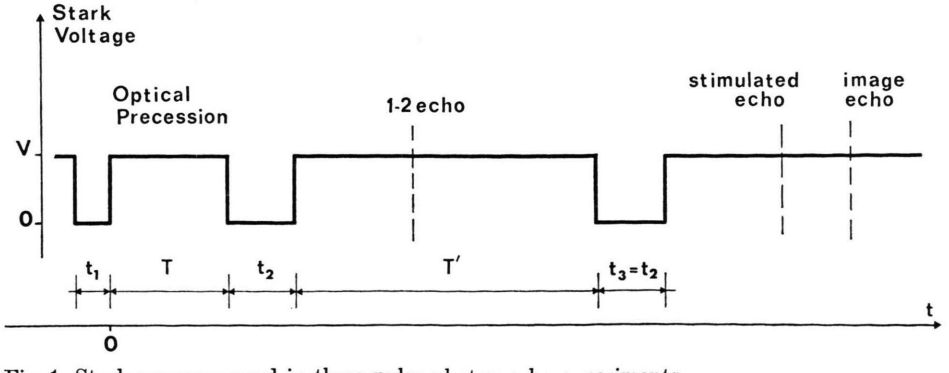

Fig. 1. Stark sequence used in three pulse photon echo experiments.

After a delay time T, a second Stark pulse (duration t_2) is applied. Precession phases are inverted and the so-called "1 – 2 echo" [8] occurs at time $t = 2T + t_2$ when the inhomogeneous dephasing Φ_i is balanced *. At the time of the echo, the precession phase of a molecular class is written as:

$$\varphi_{12}(2T + t_2) = \int_{T+t_2}^{2T+t_2} \alpha(t')\,dt' - \int_0^T \alpha(t')\,dt' = G v_y T (T + t_2). \quad (3)$$

Averaging over the velocity distribution, the reduction of the echo amplitude due to motion effects is found to be [13]

$$\langle \exp(-i\varphi_{12}) \rangle = \exp[-\tfrac{1}{4} G^2 v_0^2 T^2 (T + t_2)^2], \quad (4)$$

where v_0 is the most probable velocity. This echo, generally used to monitor coherence relaxation, is actually strongly affected by molecular motions through the inhomogeneous Stark field (damping characteristic time $\sim (G v_0)^{-1/2}$).

Let us now consider the third Stark pulse (duration $t_3 = t_2$), applied at time $t = T + T' + t_2$. Up to four echoes are induced at further times with relative amplitudes depending on pulse areas [8].

i) Two echoes appear at $t = 2(T + T' + t_2)$ and $t = T + 2(T' + t_2)$: they originate from the polarization induced respectively by the first and the second Stark pulses, and inverted by the third pulse. They are not considered further since their behaviours versus delay times are quite similar to those of usual two pulse echeos.

ii) The so called "stimulated echo" which occurs at time $t = 2T + T' + 2t_2$, originates from the polarization induced by the first Stark pulse, and inverted by a combined effect of the second and the third pulses. Between these two pulses only population relaxation is involved, so this echo has revealed to be fruitful for relaxation and velocity changing collision studies [8]. The precession phase of a molecular velocity class is written as:

$$\varphi_{st}(2T + T' + 2t_2) = \int_{T+T'+2t_2}^{2T+T'+2t_2} \alpha(t')\,dt' - \int_0^T \alpha(t')\,dt' = G v_y T (T + T' + 2t_2). \quad (5)$$

Averaging over molecular velocities, the reduction of the echo amplitude due to motion effects is written as:

$$\langle \exp(-i\varphi_{st}) \rangle = \exp[-\tfrac{1}{4} G^2 v_0^2 T^2 (T + T' + 2t_2)^2]. \quad (6)$$

iii) The so called "image echo" which occurs at time $t = 2(T' + t_2)$, is related to the "1 – 2 echo" polarization inverted by the third pulse. The precession phase of a molecular class is then:

$$\varphi_{im}(2T' + 2t_2) = \int_{T+T'+2t_2}^{2T'+2t_2} \alpha(t')\,dt' - \int_{T+t_2}^{T+T'+t_2} \alpha(t')\,dt' + \int_0^T \alpha(t')\,dt' = G v_y (T' - 2T)(T' + t_2) \quad (7)$$

and the reduction of the echo amplitude is:

$$\langle \exp(-i\varphi_{im}) \rangle = \exp[-\tfrac{1}{4} G^2 v_0^2 (T' - 2T)^2 (T' + t_2)^2]. \quad (8)$$

In the case of a Carr Purcell sequence ($T' = 2T$) [6], Eq. (8) shows that the image echo amplitude is unaffected by molecular motions. The macroscopic polarization then builds up exactly at time $t = 4T + 2t_2$, and its time behaviour only depends on coherence relaxation. Such a result holds as long as the frequency gradient G is uniform and the second and third pulse durations are equal ($t_2 = t_3$). This image echo property is well illustrated in Fig. 2 where phase deviations Φ_i and Φ_m are plotted separately for a particular molecular class. The phase deviation Φ_i, related to inhomogeneous effects (Doppler effect and molecular location at time $t = 0$), evolves linearly with time and leads obviously to a correct rephasing for each echo. The molecular motion through the inhomogeneous Stark field leads to the phase deviation $\Phi_m (\sim t^2)$. At the time of the 1 – 2 echo, the phase Φ_m depends strongly on the considered molecular class: this entails the predicted damping of (4). On the contrary, a correct rephasing occurs at the time of the image echo: this echo is then unaffected by molecular motions and can be used to monitor coherence relaxation. This property, previously observed in pulsed NMR when convection processes occur in the sample [6], can be easily generalized to a multiple-pulse Carr Purcell sequence: all the even numbered echoes are unaffected by molecular motions in the inhomogeneous Stark field.

On the other hand, it follows from Eqs. (5) and (6) that, if $T' = 2T$, the simulated echo appears simultaneously with the image echo, but its ampli-

* When the Doppler broadening prevails an extra delay related to the duration t_1 of the first pulse occurs [14, 8]. It may be neglected here owing to the leading role of the inhomogeneous Stark broadening.

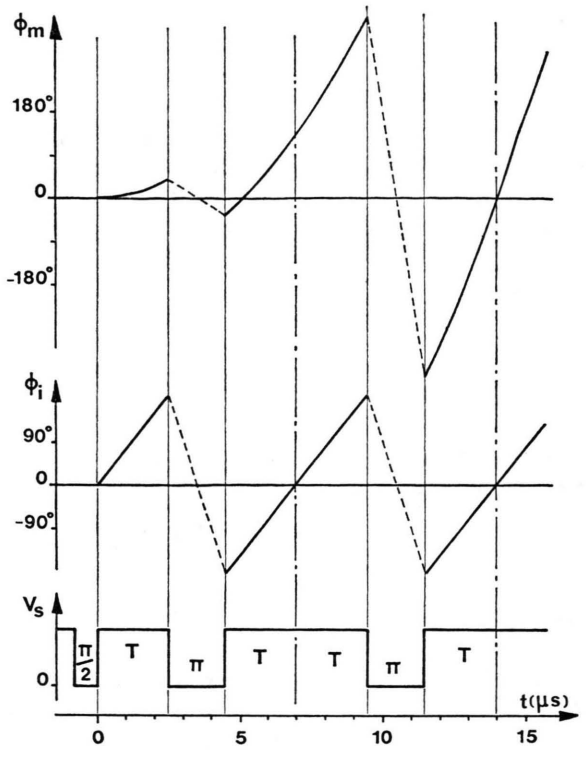

Fig. 2. Precession phase behaviour of a particular molecular class for the case of an ideal Carr Purcell sequence ($\pi/2$, π, π sequence). Φ_i is the phase deviation induced by inhomogeneous effects and is mainly related to molecular location at $t=0$. Φ_m is the phase deviation related to molecular motion in the inhomogeneous Stark field. Curves are plotted with the parameters: $G=5$ rad/μs/cm; $y=0.25$ cm; $v_y=400$ m/s; $v_z=0$. Φ_i and Φ_m are both zero at the time of the 2nd echo.

tude always remains affected by molecular motions in the inhomogeneous Stark field. Thus, using sufficiently large G values, the stimulated echo amplitude is rapidly dropped to zero with increasing delay times; moreover, if the second and third pulses are nearly π pulses, the stimulated echo amplitude is minimum whereas the image echo is maximum and thus contributes solely to the second echo [8].

III. Experimental Study

Three pulse photon echoes in inhomogeneous Stark field were observed at a 3 mm wavelength on CH_3F ($J=1\rightarrow 2$, $|KM|=1$ transition) [15]. At such a frequency, the whole Doppler profile ($\cong 110$ kHz HWHM) is easily saturated and pure nutation or precession stages are allowed.

The molecular transition used has a linear Stark effect and a uniform frequency gradien G^* was obtained in a "tilted Lide-cell" made from two copper folded plates (Figure 3). The microwave field coupling was performed with adjustable horns: good propagation conditions were obtained with a cell length limited to 50 cm. The Stark generator delivered up to 75 V pulses with about 20 ns rise and fall times. Pulse durations and delay times were adjusted with 50 ns steps by means of a 20 MHz quartz controlled TTL pulse generator.

The microwave field was supplied by a Varian klystron operating in the fundamental mode: a $\cong 10$ mW electromagnetic power was obtained in the cell, leading to a $\cong 700$ kHz saturation broadening. Slow frequency drifts were removed by a quartz controlled stabilization system: great care in its adjustment had to be taken in order to perform echo sequences as long as several 10 μs. Otherwise strong extradampings were introduced by the source bandwidth, that is when the electromagnetic field correlation time was not long enough [16].

The signal, detected by a Schottky barrier diode, was amplified and treated in a 256 – channel digital averager (minimum channel width: 10 ns; repection rate: 2.5 kHz).

All the predicted three pulse echoes were observed and the maximum amplitude of a given echo was obtained by adjusting the various pulse durations [8]. In the following, we report experiments dealing with the Carr Purcell sequence ($T'=2T$) since, as indicated before, only in this case molecular free flight effects in the inhomogeneous Stark field vanish for the image echo.

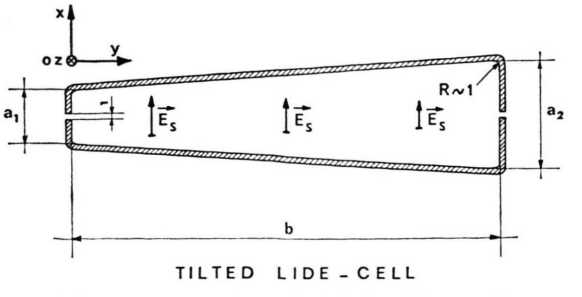

Fig. 3. Cross section of the "tilted Lide-cell". $a_1=10.8$ mm; $a_2=20.2$ mm; $b=80$ mm; cell length = 500 mm.

* A uniform frequency gradient would be obtained rigorously with a hyperbolic cross-section cell. It can be shown that the actual gradient non linearity has no influence in our experimental conditions.

A typical recording is presented in Figure 4. The optical precession induced by the first pulse, which appears as a beating between the c.w. millimeter wave and the field reemitted by the gas is rapidly damped owing to the strong Stark field inhomogeneity; its shape is fairly reproduced by echoes, but the phase is inverted after each π pulse. Large echo amplitudes were obtained when the second and third pulses are nearly π: in this case, the stimulated echo formation is reduced and the image echo is enhanced. Although these two echoes occur simultaneously with opposite phases, the stimulated echo plays no rôle in the second echo amplitude since it remains strongly damped by molecular motions in the inhomogeneous Stark field, as indicated before.

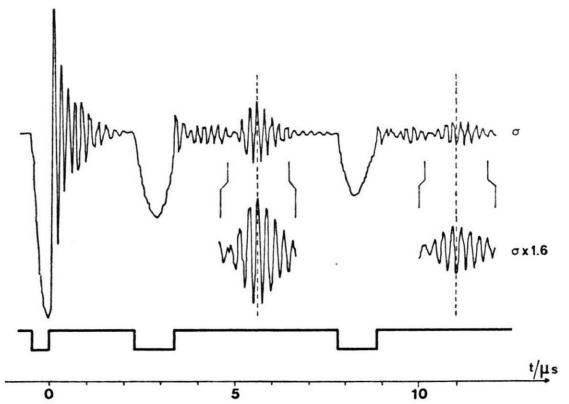

Fig. 4. Three pulse Carr Purcell sequence: pulse durations $t_1 = 0.5$ μs, $t_2 = t_3 = 1.0$ μs; Stark voltage $V \cong 28$ V; mean Stark shift $\bar{\alpha}/2\pi \cong 5.8$ MHz; frequency gradient $G \cong 2.8$ rad/μs/cm; CH_3F pressure $\cong 0.7$ m Torr; coherence relaxation time $T_2 \cong 9$ μs.

Theoretical predictions of Sect. II related to the molecular motion influence are well supported by Figure 5: for various delay times, echo amplitude behaviours are plotted versus the square of the applied Stark voltage V. The $1-2$ echo (in full lines) appears strongly affected when either the Stark field gradient or the delay time T are increased, and the theoretical law of Eq. (4) is well satisfied: straight line slopes agree within 10% with the theoretical G value deduced from the cell geometry ($G/V \cong 0.1$ rad/μs/cm/V). On the other hand, image echoes (in dotted lines) are unaffected by the molecular motions in the inhomogeneous Stark field. The slight slope actually observed has the same value whichever the delay time T is: thus, it is only related to the Stark field amplitude which fixes the optical precession frequency $\bar{\alpha}$ and does not depend on molecular motions in the inhomogeneous Stark field. This slope may originate in a cell transmission

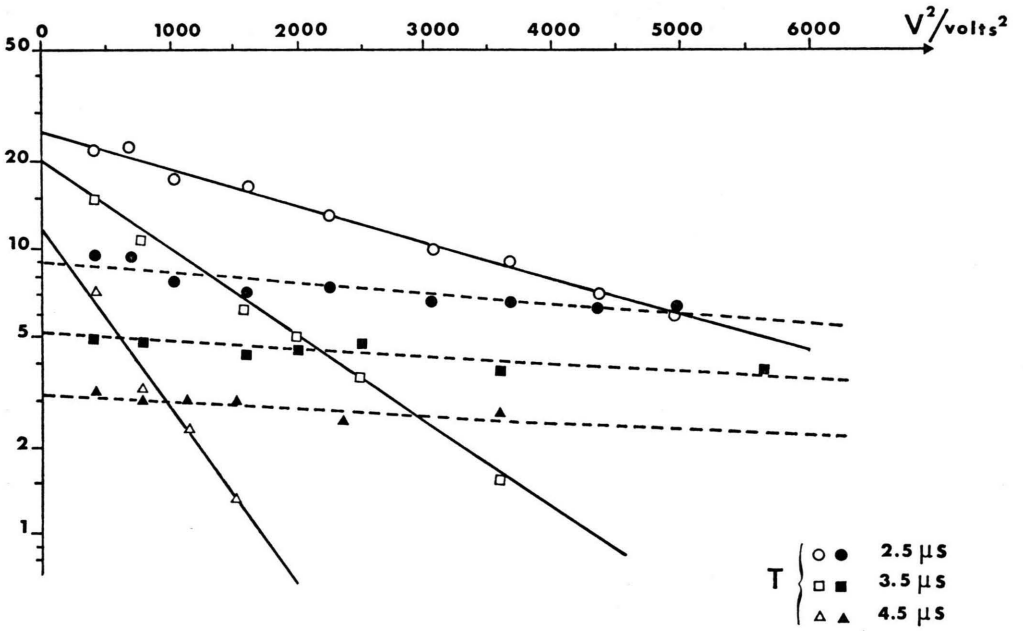

Fig. 5. Three pulse Carr Purcell sequence: amplitude behaviours of the first echo (in full line) and the second echo (in dotted line) versus the square of the applied Stark voltage V, for various delay times T. Experimental data: $t_1 = 0.5$ μs; $t_2 = t_3 = 1.0$ μs; CH_3F pressure $\cong 0.85$ m Torr; $T_2 \cong 7.5$ μs. Amplitudes are normalized to first pulse amplitudes (100).

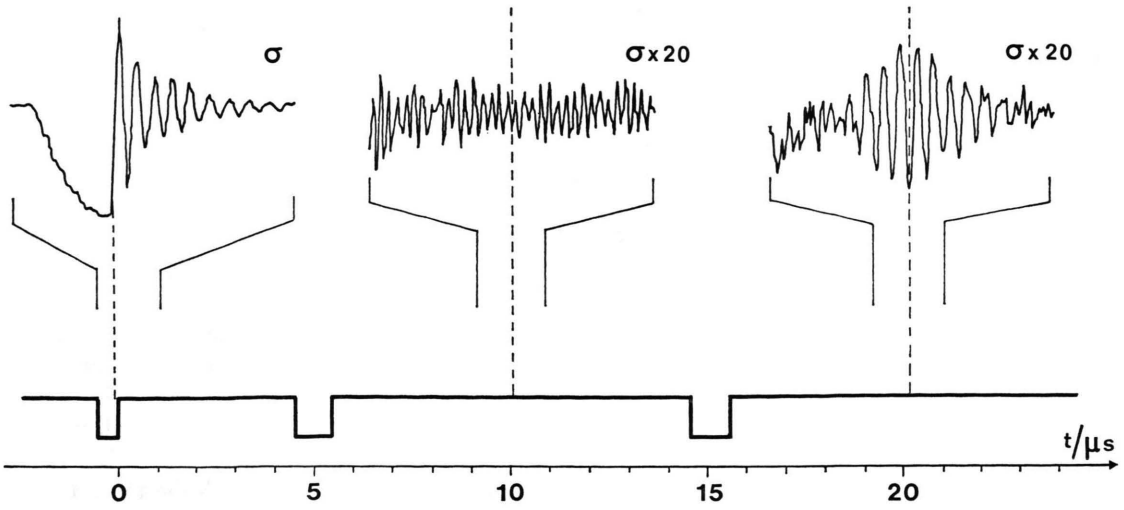

Fig. 6. Three pulse Carr Purcell sequence: the macroscopic polarization, smeared out by motional dephasing at the first echo time, builds up at the second echo time. $t_1 = 0.5\ \mu s$; $t_2 = t_3 = 1.0\ \mu s$; $V \cong 50$ V; $\overline{\alpha}/2\pi \cong 10$ MHz; $G \cong 5$ rad/μs/cm; CH_3F pressure $\cong 0.65$ m Torr; $T_2 \cong 9.5\ \mu s$.

depending on the electromagnetic field frequency (e.g. due to a small residual standing wave) or in the finite rise time of the Stark field. It may be discarded as long as experiments with various delay times are performed using the same Stark field.

As a conclusion, Fig. 5 diagram exhibits that the free flight molecular motion does not have an irreversible character like the Brownian motion involved in NMR experiments. This is clearly illustrated in Figure 6: for a long delay time and a large Stark field, the macroscopic polarization is completely destroyed at the time of the $1-2$ echo; however, the microscopic coherence still exists, and after the third Stark pulse, the polarization builds up to get the image echo, the amplitude of which only depends on pulse areas and coherence relaxation.

IV. Applications

Photon echo experiments in inhomogeneous Stark field were undertaken with the purpose of studying elastic collisions which change the molecular velocity without loss of coherence. In the infrared [7, 8, 17] and optical domains [10] these velocity changing collisions lead to large Doppler shifts which damage the echo formation: such Doppler shifts are obviously negligible in the millimetre range. On the other hand, if a strongly inhomogeneous Stark field is used, velocity changing collisions will modify the phase restoration and then the image echo amplitude. If an active molecule undergoes a velocity change Δv_y, the precession phase will undergo a change $G\,\Delta v_y\,\tau^2/2$, where τ is the time elapsed since the collision. For a time $\tau \gtrsim (2/G\,\Delta v_y)^{1/2}$, this factor is $\gtrsim 1$ radian: the molecule contribution to the echo is destroyed and the echo amplitude exhibits an extradamping of form $\exp(-\Gamma_{VC}\,t)$, where Γ_{VC} is the rate of velocity changing collisions. For shorter times, the echo behaviour may be evaluated by means of Flusberg's statistical arguments [18], especially collisions occur at random times and the velocity changes, much smaller than the most probable velocity, are uncorrelated and nearly independent of velocity. Using the Keilson-Storer collision kernel [19], a calculation similar to Flusberg's one gives an image echo damping of form $\exp\left(-\frac{17}{20}\,\Gamma_{VC}\,G^2\,\overline{\Delta v^2}\,T^5\right)$ where T is the 1st – 2nd pulse delay time and $\overline{\Delta v^2}$ the mean square value of velocity change per collision. This T^5 law, which differs from the T^3 law obtained for Doppler broadened lines [7, 18], originates in the spatial nature of the inhomogeneous broadening considered. No experimental evidence for these laws was observed with our present experimental conditions ($G \leqq 8$ rad/μs/cm, $4\,T \leqq 50\ \mu s$): for the $(J, |K\,M| = 1, 1 \rightarrow 2, 1)$ transition of CH_3F, an upper limit for velocity change per collision can then be estimated

to be $\cong 10$ m/s, a result consistent with the 0.85 m/s value obtained by infrared measurements [17] on the same molecule.

The previous study shows that the image echo is affected neither by velocity changing collisions nor by motion effects and it is then useful for measuring coherence relaxation times T_2 which could be derived neither from optical precession nor from conventional photon echoes.

It can be shown that the relative amplitude of the image echo, compared to the first pulse amplitude, may be written as [20]:

$$\eta = A(\theta_1, \theta_2, \theta_3) \exp\left(-\frac{t}{T_2} - \frac{t}{\tau_w} - \frac{t^2}{\tau_{tr}^2}\right). \quad (9)$$

τ_w accounts for wall collisions: in a rectangular waveguide, $\tau_w = a\sqrt{\pi}/v_0$ [21], where a is the small cell dimension, assumed much shorter than the other ones. $A(\theta_1, \theta_2, \theta_3)$ and τ_{tr} characterize the echo amplitude reduction involved both by the actual pulse areas θ_i and by the transverse structure of the e.m. field. Theoretical calculations [20] allow us to determine these two quantities by solving the Bloch-Maxwell equations [22] and projecting the induced gas polarization on the propagation mode used [23, 21]. It is found that $A(\theta_1, \theta_2, \theta_3)$ only depends on the pulse areas $\theta_i = \mu E_0 t_i/\hbar$ (E_0: maximum electromagnetic field amplitude), but is always smaller than 1: on account of the transverse structure of the microwave field, molecules are submitted to pulses of various areas according to their locations so that a complete restoration of the macroscopic polarization can never be reached. Moreover, a given molecule as it moves through the electromagnetic beam is submitted to pulses with various coupling strengths: this entails an extra damping time τ_{tr} which appears as a residual Doppler effect, a well-known process in saturated absorption laser spectroscopy [24]. In the case of a TE_{01} mode $\tau_{tr} \cong 2b/\pi v_0$ [20], where b is the width of the waveguide.

Image echo amplitudes, measured for sequence durations from 6 μs up to several 10 μs, for various pressures in the range 0.2 – 2.5 m Torr, are reported in Figure 7. The quoted values are in fact corrected from the residual Doppler effect: for this purpose, an effective mode width $b^* \cong 40$ mm ($\tau_{tr} \cong 67$ μs) was deduced from the damping time $2\pi/Gb$ of the optical precession. For the sake of comparison, amplitudes are given as a function of the first pulse amplitude, the other experimental parameters,

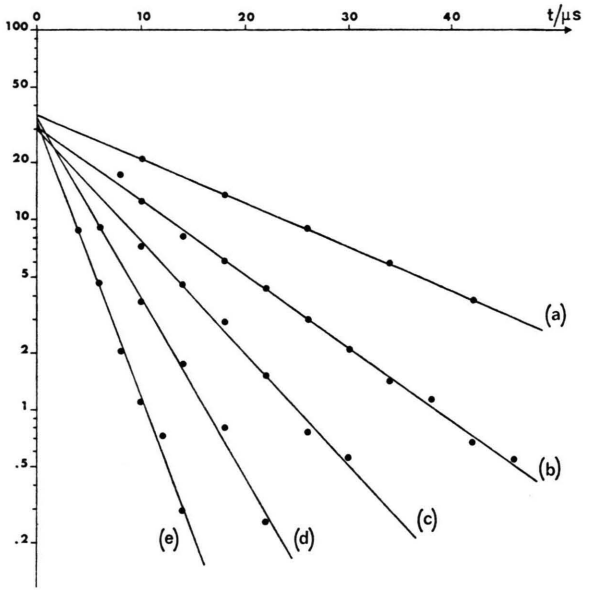

Fig. 7. Behaviours of the image echo amplitude versus time for various CH_3F pressure (in m Torr): 0.26 (a), 0.47 (b), 0.95 (c), 1.50 (d), 2.56 (e). Amplitudes are normalized to first pulse amplitudes (100). Experimental data: $t_1 = 0.4$ μs; $t_2 = t_3 = 1.0$ μs; saturation broadening $\cong 700$ kHz; $V \cong 28$V.

namely the Stark field, the electromagnetic field amplitude and excitation pulse areas, being kept constant.

Echo amplitude behaviour fairly agree with Eq. (9) and line slopes give a measurement of the coherence relaxation time $(1/T_2 + 1/\tau_w)^{-1}$. It is interesting to note that zero time intercepts occur in the 30 – 35% range, whichever the pressure is. This value, which, as expected, is nearly constant, characterizes the efficiency factor $A(\theta_1, \theta_2, \theta_3)$ of the echo sequence. However it is smaller than the theoretical value corresponding to our experimental conditions ($\cong 60\%$), probably because of residual standing waves and of an actual propagation mode different from a TE_{01} one.

At least, we have deduced from these measurements the coherence relaxation time T_2 of the $(J, |KM| = 1, 1 \rightarrow 2, 1)$ transition of CH_3F at room temperature ($\cong 300$ K). For the sake of comparison, the population relaxation time T_1 was measured by a delayed nutation technique [7] during the same cycle of experiments and using the same capacitance pressure gauge (Datametrics 573 A-1 T). The line broadenings associated to the population and coherence relaxations are given by:

$\Delta\nu_1 = (18.8 \pm 1.0)\,\mathrm{kHz/m\,Torr} \cdot p + (2.1 \pm 1.2)\,\mathrm{kHz}$,
$\Delta\nu_2 = (19.7 \pm 1.4)\,\mathrm{kHz/m\,Torr} \cdot p + (4.1 \pm 1.6)\,\mathrm{kHz}$,

where p is the sample pressure. Quoted errors are twice standard deviations. Zero pressure intercepts related to wall collisions are in good agreement with the theoretical value [21] $(2\pi\tau_w)^{-1} = v_0/2a\pi^{3/2} \cong 2.3$ kHz ($a = 15$ mm, the mean value of the small cell dimension).

The obtained relaxation times $T_1 = (8.5 \pm 0.4)\,\mu\mathrm{s} \cdot \mathrm{m\,Torr}$ and $T_2 = (8.1 \pm 0.5)\,\mu\mathrm{s} \cdot \mathrm{m\,Torr}$ are nearly equal. This result is in agreement with other studies of rotational relaxation in CH_3F, which indicate that $T_1 = T_2$ [25, 7], that is phase changing collisions are negligible [7].

Acknowledgements

The authors wish to thank J. M. Carpentier and J. P. Prault for their assistance with the experimental measurements.

[1] N. A. Kurnit, I. D. Abella, and S. R. Hartmann, Phys. Rev. Lett. **13**, 567 (1964); I. D. Abella, N. A. Kurnit, and S. R. Hartmann, Phys. Rev. **141**, 391 (1966).
[2] J. L. Jenkins and P. E. Wagner, Appl. Phys. Lett. **13**, 308 (1968).
[3] C. K. N. Patel and R. E. Slusher, Phys. Rev. Lett. **20**, 1087 (1968).
[4] B. Bölger and J. C. Diels, Phys. Lett. **28 A**, 401 (1968).
[5] E. L. Hahn, Phys. Rev. **80**, 580 (1950).
[6] H. Y. Carr and E. M. Purcell, Phys. Rev. **94**, 630 (1954).
[7] P. R. Berman, J. M. Levy, and R. G. Brewer, Phys. Rev. **A11**, 1668 (1975).
[8] R. L. Shoemaker, in "Laser and Coherence Spectroscopy", edited by J. I. Steinfeld, Plenum Press, New York 1978, p. 197.
[9] T. Mossberg, A. Flusberg, R. Kachru, and S. R. Hartmann, Phys. Rev. Lett. **42**, 1665 (1979).
[10] T. W. Mossberg, R. Kachru, and S. R. Hartmann, Phys. Rev. Lett. **44**, 73 (1980).
[11] R. H. Schwendeman, Ann. Rev. Phys. Chem. **29**, 537 (1978).
[12] P. Glorieux, J. Legrand, and B. Macke, J. Physique **36**, 643 (1975).
[13] P. Glorieux, J. Legrand, and B. Macke, Chem. Phys. Lett. **40**, 287 (1976).
[14] L. Allen and J. H. Eberly, Optical Resonance and Two-Level Atoms, John Wiley and Sons, New York 1975.
[15] P. A. Steiner and W. Gordy, J. Mol. Spect. **21**, 291 (1966).
[16] F. Rohart and B. Macke, Appl. Phys. (1981) in press.
[17] B. Comaskey, R. E. Scotti, and R. L. Shoemaker, Opt. Lett. **6**, 45 (1981).
[18] A. Flusberg, Opt. Commun. **29**, 123 (1979).
[19] J. Keilson and J. E. Storer, Q. Appl. Math. **10**, 243 (1952).
[20] F. Rohart, Internal Report LSH 1968-18 (May 1981) Available on request.
[21] H. Mäder, Z. Naturforsch. **34a**, 1170 (1979).
[22] C. L. Tang and B. D. Silverman, in "Physics of Quantum Electronics", edited by P. Kelley, B. Lax, and P. E. Tannenwald, Mac Graw Hill, New York 1966, p. 280.
[23] F. Rohart, P. Glorieux, and B. Macke, J. Phys. B: Atom. Molec. Phys. **10**, 3835 (1977).
[24] C. J. Bordé, J. L. Hall, C. V. Kunasz, and D. G. Hummer, Phys. Rev. **A14**, 236 (1976).
[25] H. Jetter, E. F. Pearson, C. L. Norris, J. C. McGurk, and W. H. Flygare, J. Chem. Phys. **59**, 1796 (1973).